NASA TECHNICAL MEMORANDUM

NASA TM X-53329

September 13, 1965

NASA TM X-53329

EXPERIMENTAL X-RAY STRESS ANALYSIS FOR PRECIPITATION HARDENED ALUMINUM ALLOYS

By James H. Wharton and William L. Prince
Propulsion and Vehicle Engineering Laboratory

NASA

George C. Marshall Space Flight Center, Huntsville, Alabama

September 13, 1965 NASA TM X-53329

EXPERIMENTAL X-RAY STRESS ANALYSIS FOR PRECIPITATION HARDENED ALUMINUM ALLOYS

By James H. Wharton and William L. Prince

George C. Marshall Space Flight Center
Huntsville, Alabama

ABSTRACT

X-ray diffraction techniques for determining stress in precipitation hardened aluminum alloys have been developed and evaluated. The materials investigated included 2014-T6, 2219-T37, and 7075-T6 aluminum alloys. A precision corresponding to ± 5 percent of the alloy yield strengths was obtained under laboratory conditions. Further studies are needed to evaluate this method for field measurements of stress in vehicle components.

NASA - GEORGE C. MARSHALL SPACE FLIGHT CENTER

NASA - GEORGE C. MARSHALL SPACE FLIGHT CENTER

TECHNICAL MEMORANDUM X-53329

EXPERIMENTAL X-RAY STRESS ANALYSIS FOR PRECIPITATION HARDENED ALUMINUM ALLOYS

By James H. Wharton and William L. Prince

PROPULSION AND VEHICLE ENGINEERING LABORATORY

TABLE OF CONTENTS

LIST OF ILLUSTRATIONS

EXPERIMENTAL X-RAY STRESS ANALYSIS FOR PRECIPITATION HARDENED ALUMINUM ALLOYS

By James H. Wharton and William L. Prince
George C. Marshall Space Flight Center

SUMMARY

X-ray diffraction techniques for determining stress in precipitation hardened aluminum alloys have been developed and evaluated. Aluminum alloys 2014-T6, 2219-T37, and 7075-T6 were investigated. Satisfactory results were obtained by the two-exposure technique for both the diffractometer and photographic methods of analysis. A precision corresponding to approximately ± 5 percent of the alloy yield strength was obtained for each alloy studied under laboratory conditions. Problems which would be expected in using this method for field analyses on production components are discussed. In general, it appears that the accuracy of the method may vary with the particular component or material and that reliability factors cannot be established without additional experimentation.

INTRODUCTION

Frequently, failures of high strength aluminum alloys have been attributed to residual and continuously applied stresses in these materials. Therefore, it is desirable in failure analysis, and especially failure prevention, to be able to determine the stress condition of materials by a nondestructive technique. X-ray diffraction techniques show promise for nondestructive stress determination, and considerable effort, especially for the steels, has been devoted to developing these techniques by various investigators (ref. 1, 2, 3, 4, 5, & 6). These investigations generally have been academic studies of stress and strain; i.e., the experiments have been artificially simplified with respect to samples and equipment. Therefore, the accuracy of X-ray techniques for measuring stress on field specimens is still uncertain.

Accordingly, a two-phase program was undertaken to determine the feasibility of X-ray stress measurements for aluminum alloy components having various compositions, heat treatments, sizes, and geometric designs. As the initial phase of this program, stress studies of commercial aluminum alloys were conducted with a standard laboratory X-ray generator using diffractometer and photographic techniques. The results of these studies are reported herein. The second phase of the program will consist of additional laboratory studies and also will include studies of actual components under field conditions.

The authors wish to express their appreciation to Messrs. James E. McDonald and Ellis L. Smith of the Structures Division, Propulsion and Vehicle Engineering Laboratory, for mounting strain gauges and to the following employees of the Materials Division, Propulsion and Vehicle Engineering Laboratory: Mr. Gordon R. Marsh of the Chemistry Branch for his assistance in the literature survey and his many other contributions; Mr. Robert L. Gilbreath of the Development Shop (R-P&VE-ME) for his aid in the design of special fixtures; and the personnel of the Metallic Materials Branch (R-P&VE-MM) for assistance in calibrating the strain gauges.

THEORY

When a polycrystalline material is deformed elastically in such a manner that the strain is uniform, the lattice plane spacings in the grains change from their strain-free distance to some new value proportional to the strain. Measurement of these changes in lattice spacings by X-ray diffraction is then a strain measurement where the lattice spacings serve as internal strain gauges. From the strain, measured by the shift in 2θ or lattice spacing, the stress present may be ascertained either from calculations involving the elastic constants or from calibration procedures using known stress values.

Unfortunately, the lattice planes perpendicular to the desired directional stress cannot be studied since these planes also are perpendicular to the sample surface. Measurements can be made for lattice planes which lie at some angle ($\psi < 90°$) to the surface, and, if ψ is greater than zero, the lattice spacings will be acted upon by a component of the directional stress. However, stress determinations should not be made from a single measurement or exposure at an angle ψ because the given lattice spacings are affected by other stresses which are apt to be in different directions from the direction the measurement was made. Consideration of the biaxial stress system makes it imperative that stresses other than that desired be eliminated. To make this correction, two measurements are required, and calculations of stress are based upon the difference in the spacings or angles measured.

In practice, the desired directional stress in the plane of and parallel to the specimen surface is determined from one exposure with the diffractometer aligned in the normal position and a second exposure with the sample inclined at an angle ψ from the normal position. The pertinent geometry for the diffractometer technique is shown schematically in FIG 1.

From fundamental elasticity theory, the difference in two theta angle $(2\theta_n - 2\theta\psi)$ is related to the component of stress by the following expression:

$$\sigma\phi = \frac{\cot\theta}{2}\left(\frac{E}{1+\mu}\right)\left(\frac{1}{\sin^2\psi}\right)(2\theta_n - 2\theta\psi) \qquad (1)$$

where $\sigma\phi$ is the component of stress in the ϕ direction, E is the elastic modulus, and μ is Poisson's ratio. If $\cot\theta$ is taken as constant over the brief range, equation 1 reduces to the linear form:

$$\sigma\phi = K_{(hkl)}\ (2\theta_n - 2\theta\psi) \qquad (2)$$

where $K_{(hkl)}$ is the stress factor and is constant for a given set of (hkl) planes in a crystalline material. The linearity of equation 2 provides a check of the validity of any given set of data since nonlinear behavior would be expected only when the elastic range for a given material is exceeded.

Although the stress factor can be calculated directly from equation 1, this procedure is generally unsatisfactory because the elastic modulus associated with a given lattice direction usually is unknown. For this reason, most investigators determine the stress factor empirically by using equation 2. For a more thorough review of the direct calculation technique, Taylor has reviewed the elastic constants to be used in stress determinations (ref. 7).

For application in the photographic technique, equation 1 may be transformed by simple trigonometric relations to give the following:

$$\sigma\phi = \frac{E}{2D(1+\mu)\ \sec^2 2\theta\ \tan\theta\ \sin^2\psi}(S_i - S_n) \qquad (3)$$

where S_i and S_n are the Debye-ring radii in the inclined and normal positions; D is the specimen-to-film distance, and the remaining parameters are consistent with equation 1. If θ is taken as constant over the brief range, equation 3 reduces to:

$$\sigma\phi = K_{(hkl)D}\ (S_i - S_n) \qquad (4)$$

where $K_{(hkl)D}$ is the stress factor for the (hkl) planes at a given D.

Although equations 1 and 3 are not often applied directly to stress determinations, these relations can be used to obtain optimum experimental conditions. For example, differentiation of the relations with respect to θ shows that greater shifts and, therefore, greater precision will be

observed as θ approaches 90°. These relations also indicate that materials having low elastic moduli will show greater shifts. Thus, stress determinations for aluminum generally should be more accurate in terms of psi than those for steel. Other material properties which affect the accuracy of X-ray stress techniques will be discussed in the following section.

EFFECTS OF PROPERTIES OF MATERIALS

Stress analyses have been conducted on 2219-T37, 2014-T6, and 7075-T6 aluminum alloys. Figure 2 shows the X-ray reflection spectra for the (422) aluminum planes measured in the normal position for these alloys. As has been reported by other workers, these alloys show considerable line broadening, which results from the coherency strains caused by precipitation reactions. Preston has studied the relation between line broadening and coherency strains in aluminum-four percent copper alloys (ref. 8).

Although the precipitates are important in considerations of the alloy properties, the most significant effect for stress studies is the loss in line definition due to the poorly resolved peaks. Referring again to FIG 2, one can correlate the degree of line broadening with the composition and metallurgical condition of the sample. The 2014-T6 alloy shows some line broadening; the 2219-T37 alloy shows extensive line broadening, and the 7075-T6 alloy gives a fairly sharp spectrum. In the age-hardened 2014-T6 alloy, the copper precipitates in thin zones (G. P. Zones) along the (100) planes of aluminum, which results in rather high coherency strains. This also takes place with the 2219-T37 but not to the same extent as for the age-hardened temper; for the -T37 temper, the extensive line broadening is mostly the result of cold working. The X-ray spectra of cold worked metals have been studied by Wood and Smith (ref. 9 and 10). Zinc precipitation in the 7075-T6 alloy results in lower coherency strains due to the geometric shape of the precipitates. Actually, a large portion of the line broadening in the 7075 alloy may be accounted for by the 1.5 percent copper content. Little mention has been made of the other components of these alloys (magnesium, silicon, and chromium) because the observed X-ray spectra can be adequately explained on the basis of copper and zinc precipitates and to include the other alloying constituents would unnecessarily complicate the description.

The grain size is as important to stress measurement as composition and temper. If the grain size tends to be coarse, the diffraction circles will be spotty, and the resultant stress determination will not be accurate. In addition to the loss in angle or line clarity, microstresses superimposed upon macrostresses for a nonstatistical number of grains may produce inconsistent experimental results.

APPARATUS

In this investigation, several techniques for uniaxial straining of test specimens were evaluated. Figure 3 shows the tensile straining device which produced the most consistent experimental data. Notice the steel back support which prevents flexing of the holder and specimen. The actual stress at the surfaces of the test specimens was obtained by strain readings from calibrated wire resistance SR-4 type strain gauges. Readings taken on both sides of the specimen agreed to within 1000 psi. Most of this differential resulted from a slight curvature of the sample, which was removed upon loading. For perfectly flat specimens, the differential was less than 500 psi, which is well within other errors in the technique. X-ray measurements were made with the Philips Norelco diffractometer and generator using a scintillation detector.

For the photographic portion of this investigation, a four-inch by five-inch back reflection camera with ± 5 degrees oscillatory motion was designed. A two-millimeter beam collimator was used to vary the film-to-sample distance without focusing considerations. In FIG 4, the photographic experimental arrangement is shown.

EXPERIMENTAL PROCEDURES

Diffractometer Method

In this method, a known stress is applied to an appropriate sample, and the corresponding difference between 2θ in the normal and 45-degree positions is measured. The stress factor $K_{(hkl)}$ is determined subsequently from a plot of stress versus $\Delta 2\theta$. Residual stress, if present, is given by the intercept.

Copper Kα radiation filtered by nickel foil was used. Peak to background ratios varied with the type of alloys from 1:1 for 2219-T37 to 3:1 for 7075-T6. The (422) aluminum line was used in the diffractometer technique. The 2θ angle for this line is the highest angle that could be recorded without mechanical interferences in the goniometer mechanism.

In the diffractometer measurements, rotation of the sample from the normal to the 45-degree position (as seen in FIG 1b) causes the focal point to be shifted away from the receiving slit. This produces artificial broadening to the oblique measurement and may produce a shift in peak position. Ideally, the solution to the problem is to move the receiving slit and detector to the new focal point; however, with most commercial diffractometers, this adjustment cannot be made reproducibily. Ogilvie suggests mounting a

receiving slit at the focal point for the oblique measurement (ref. 1). Although this procedure did reduce scattered radiation, the line broadening, when added to that inherently present, was intolerable. To solve this problem, a short three-millimeter collimator was used on the emitting source, and a one-degree receiving slit was used to compensate for the loss in intensity. This procedure is a slight variation of the one described by Maloof (ref. 11). The receiving slit and detector subsequently were moved to the optimum position, and the goniometer was aligned and calibrated.

With these instrument conditions, five sets of five samples each of 2014-T6, 2219-T37, and 7075-T6 alloys were stressed to various levels, and measurements of 2θ were made in the oblique and normal positions. Analysis of the data indicated a constant error between the normal and oblique measurements in addition to varying residual stress. This error was traced to a slight amount of mechanical play in the collimator.

To recheck the stress factors as determined above, the collimator was corrected, and the instrument was realigned and calibrated. A silicon powder spectrum was measured in the normal and 45-degree position for the (533) reflection, which coincides with the (422) aluminum line. From a series of ten measurements in each position, 2θ in the 45-degree position was measured to be 0.07 ± 0.02 degrees higher than 2θ in the normal position. The measurements for 2014-T6 were repeated on samples having essentially zero residual stress as determined from the no-load measurements. Analysis of this data gave the same stress factor as the previous measurements on 2014-T6, which indicated that the error between 2θ in the normal and 45-degree position was constant for different levels of stress. Therefore, the value of 0.07 was applied as a correction to the results for the stressed samples.

As illustrated in FIG 2, the diffraction peaks were much too broad to read visually the 2θ angles with the required precision and reproducibility. Extrapolation of the linear portion on each side of the peak to the point of intersection gave results which were reproducible to within ± 0.02 degrees when scanning at 1/8 degree per minute. For 2014-T6 and 7075-T6, only the $K\alpha_2$ peak was included; however, in 2219-T37, the $K\alpha_1$ and $K\alpha_2$ peaks were not resolved, so the two were read as one peak. This method of determining 2θ assumes that only reproducibility in reading is required since differences in 2θ are used in the final analysis.

Photographic Method

Photographic stress measurements were conducted on 2014-T6 alloy. A four-inch by five-inch film holder which was continuously oscillated through 10 degrees was located 120 ± 1 millimeters from the specimen. Both the normal and 45-degree exposure were registered on one film by using the opaque film cover shown in FIG 4.

A stress-free powdered silver sample was used as a standard. Since the problem of mechanical interferences does not exist in the photographic method, all measurements were normalized to the radius of the (511) and (333) silver reflection (46.84 millimeters with the foregoing experimental conditions). The difference was subtracted from the silver radius to obtain the aluminum radius. Since the breadth of the patterns varied from specimen to specimen and with stress, the reproducibility varied from $\pm$0.2 millimeter up to unmeasurable films. Normally, the films could be read to within $\pm$0.3 millimeter as determined by three readings for each exposure. A typical pattern is shown in FIG 5.

RESULTS

Figure 6 shows the $\Delta 2\theta$ shifts versus the applied stress for three 2014-T6 samples. Failure of the lines to pass through the origin is the result of different residual stresses. Normalization of the individual curves to zero intercept by vertical displacement is shown in FIG 7 in which the data from five different samples are fitted by a single straight line passing through the origin. Figure 8 shows the $\Delta 2\theta$ versus applied stress for selected 2014-T6 samples which had essentially zero residual stress and, therefore, did not have to be normalized. The stress factor for 2014-T6 alloy was 62.5 ksi/degree from FIG 7 and 62.9 ksi/degree from FIG 8. This agreement is well within the experimental error. Standard deviations from the least squares curves in terms of stress are $\pm$3.1 ksi from FIG 7 and $\pm$2.5 ksi from FIG 8.

Figures 9 and 10 present the normalized data for 2219-T37 and 7075-T6, respectively. For 2219-T37, the stress factor was measured to be 61.7 ksi/degree, and the standard deviation of the points from the least squares curve in terms of stress was $\pm$2.0 ksi. For 7075-T6 alloy, the stress factor was 50.7 ksi/degree, and the corresponding standard deviation was $\pm$3.3 ksi.

Photographic data for 2014-T6 are shown in FIG 11 and FIG 12. These data are similar to the diffractometry data shown in FIG 6 and FIG 7 and indicate a stress factor of 6.9 ksi/millimeter with a standard deviation of $\pm$3.1 ksi.

These data indicate that stress levels in laboratory rolled sheet specimens can be reproducibly and accurately measured by diffractometer or photographic X-ray techniques. For the laboratory standards used in this work, the standard deviations corresponded to approximately $\pm$5 percent of the yield strengths of the different alloys.

As indicated above, normalization of the data shown in FIG 7, 9, 10, and 12 was accomplished by vertical displacement which effectively adjusts the data to zero residual stress. For 2014-T6 alloy, residual stresses

for individual specimens ranged from -5.1 to +3.1 ksi, with negative values indicating compressive stresses. For 2219-T37 and 7075-T6 alloys, the corresponding ranges were -5.1 to +0.5 ksi and -2.5 to +1.7 ksi, respectively. Results for other specimens of 2014-T6 alloy (not included in the various figures) have indicated residual stresses in excess of 11 ksi for .090-inch thick material. The precision with which residual stresses can be determined by this method is approximately the same as that for applied stresses, i.e., approximately ± 5 percent of the alloy yield strength.

DISCUSSION

For field applications, a single $\Delta 2\theta$ value will be obtained and multiplied by the stress factor for the particular alloy to determine total stress (applied plus residual) in the component. In the event that no external load is imposed on the component, the determined stress will correspond to the residual stress.

The accuracy of X-ray measurements can be improved by utilizing more elaborate and refined methods than were used in this work. In general, absolute peak positions can be determined more precisely by fixed counting techniques through the 2θ range and subsequently using the parabolic fitting method described by Ogilvie (ref. 1) to determine peak positions. Further corrections which take into account asymmetry of the peaks due to intensity factors have been described by Koistinen and Marburger (ref. 12 and 13). These corrections were not used in this work because the partially resolved $K\alpha_2$ peak produces an asymmetry in the $K\alpha_1$ peak which would necessitate applying the parabolic fitting method to both peaks to locate the true maximum of the $K\alpha_1$ peak. This would introduce considerable mathematical complexity to the stress measurements and probably would not greatly improve the accuracy.

From the discussion thus far, it is evident that for simple laboratory samples stress measurements by X-ray diffraction are straightforward and the accuracy attainable is within usable limits. However, the determination of stress in production components is complicated by a number of problems, especially under field conditions.

These problems can be divided into three categories: problems associated with the internal structure of the material, problems associated with the geometric design and size of a component, and problems associated with the measuring equipment.

Probably the most difficult to overcome are the problems associated with internal materials properties. Because the stress factor will vary with the thermal exposure, degree of cold working, and other factors, it

is desirable that the metallurgical state of the component alloy be identical to the metallurgical state of the standards. Additional studies are needed to determine the magnitude of errors associated with variations in metallurgical state.

With respect to the geometrical design of a component, there should be at least one square inch of flat surface which is accessible with a back reflection camera. In addition, there should be provision for mounting the camera for the vertical and oblique exposures on very large assemblies. For large grain alloys such as the aluminum castings, either the component or the camera must be oscillated and vibrated to average the grain effects.

In field applications of stress measurements, the components to be analyzed usually cannot be manipulated as small scale laboratory samples. Portability and extreme maneuverability, coupled with precision, become essential to the X-ray apparatus. Weaver and Rose (ref. 14) have designed a portable back reflection camera which can be oscillated through a few degrees in its plane about the incident beam for field stress analyses. In the present study, oscillation of the film helped to smooth the texture in most cases; however, four of ten 2014-T6 samples produced unsuitable patterns. Not only were the films spotty and broad because of different strains in individual grains but additional broadening occurred due to plastic deformation of a few grains at stress levels within 25 percent of the yield point.

The control of film-to-specimen distance and the control of the angle of incidence of the X-ray beam are as important as portability and maneuverability. If standards are used to calibrate the film, the film-to-specimen distance should be controlled to one part per thousand. Without standards, the distance should be controlled even more precisely. In all cases, standards should be utilized for film reading purposes. Control of the incident angle is not as critical as one might expect. According to equation 1, an error of 0.5 degree in the incident angle corresponds to an error of two percent in stress at 45 degrees. However, focusing considerations may result in larger errors than predicted from theory. It is essential that the pivot point of rotation be at the specimen surface since rotation to the oblique position changes the film-to-specimen distance and the area being X-rayed. In this work, variation of the sample surface from the pivot point by 0.05 inch resulted in a 3,000 psi error for the 2014-T6 alloy. Although this error seems high for the slight displacement, the effect was observed repeatedly. Correction of the alignment removed the effect.

From the foregoing discussion, one can conclude that X-ray measurement of stress under field conditions will require instrumentation having portability, maneuverability, special mounting jigs for various sample configurations, accurate controls for distances and angles, an oscillating

film holder in the camera, and a variable aperture for focusing. Commercial instrumentation is available with some of these features; however, no one system currently provides all of the necessary features.

CONCLUSIONS

X-ray diffraction techniques permit laboratory determinations of stresses in 2014-T6, 2219-T37, and 7075-T6 aluminum alloys with an accuracy of ± 5 percent of the yield strength. These techniques of measuring stresses should prove quite useful in research and development programs where suitable control can be maintained over samples and equipment and where wire resistance strain gauges are not applicable.

Extension of the X-ray stress technique to field problems involving production components will be more difficult, especially for the precipitation hardened aluminum alloys where wide fluctuations in the metallurgical state may be expected. The accuracy of field measurements for a particular component cannot be determined without additional investigation.

REFERENCES

1. Ogilvie, R. E.: Stress Measurements With X-ray Spectrometer. M. S. Thesis, Massachusetts Institute of Technology, 1952.

2. Wood, W. A.: The Behaviour of the Lattice of Polycrystalline Iron in Tension. Proc. Roy. Soc., series A, vol. 192, 1948, pp. 218-231.

3. Smith, L. S.; and Wood, W. A.: A Stress-Strain Curve for Mild Steel and the Physical Significance of the Yield Point of a Metal. Proc. Roy. Soc., series A, vol. 179, 1942, pp. 450-460.

4. Christenson, A. L.; and Rowland, E. S.: X-ray Measurement of Residual Stress in Hardened High Carbon Steel. Transactions A.S.M., vol. 45, 1953, pp. 638-676.

5. Cullity, B. D.: Elements of X-ray Diffraction. Addison Wesely Publishing Company, Inc., 1956.

6. Barrett, C. S.: Structure of Metals. McGraw-Hill Book Company, Inc., 1952.

7. Taylor, A.: X-ray Metallograph. John Wiley and Sons, Inc., 1961.

8. Preston, G. D.: Precipitation in the Solid State. J. Sci. Instr., vol. 18, 1941, pp. 154-157.

9. Wood, W. A.: The Lower Limiting Crystalline Size and Internal Strains in Some Cold-Worked Metals. Proc. Roy. Soc., series A, vol. 172, 1939, pp. 231-241.

10. Wood, W. A.; and Smith, S. L.: Behaviour of the Crystalline Structure of Brass Under Slow and Rapid Cyclic Stresses. Proc. Roy. Soc., series A, vol. 174, 1940, pp. 310-321.

11. Maloof, S. R.: X-ray Strain Measurement Techniques With a Norelco Wide-Range X-ray Diffractometer. Norelco Reporter, vol. 1, no. 3, 1954, p. 35.

12. Koistinen, D. P.; and Marburger, R. E.: X-ray Measurement of Residual Stresses in Hardened Steels. Proceedings of the Symposium on Internal Stresses and Fatigue in Metals, 1958, pp. 08-109.

13. Koistinen, D. P.; and Marburger, R. E.: A Simplified Procedure for Calculating Peak Position in X-ray Residual Stress Measurements on Hardened Steels. Transactions A.S.M., vol. 51, 1959, pp. 537-555.

14. Weaver, F.; and Rose, A.: Mitt. Kaiser-Wilhelm Inst. Eisenforsch. Düsseldorf, vol. 17, 1935, p. 33.

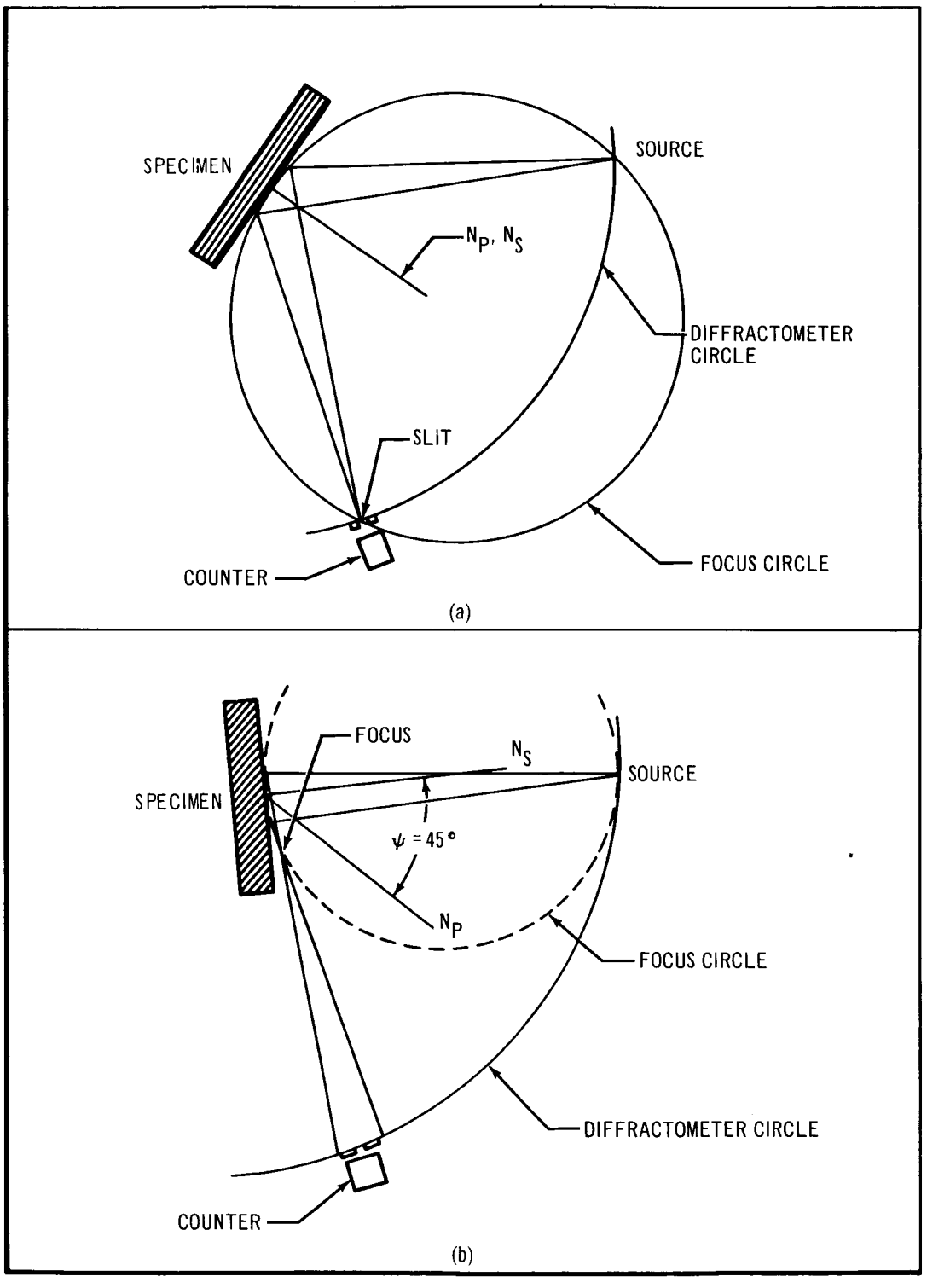

FIGURE 1.- GEOMETRICAL ILLUSTRATION OF THE DIFFRACTOMETER TECHNIQUE IN STRESS MEASUREMENTS: (a) $\psi = 0$ (b) $\psi = 45°$

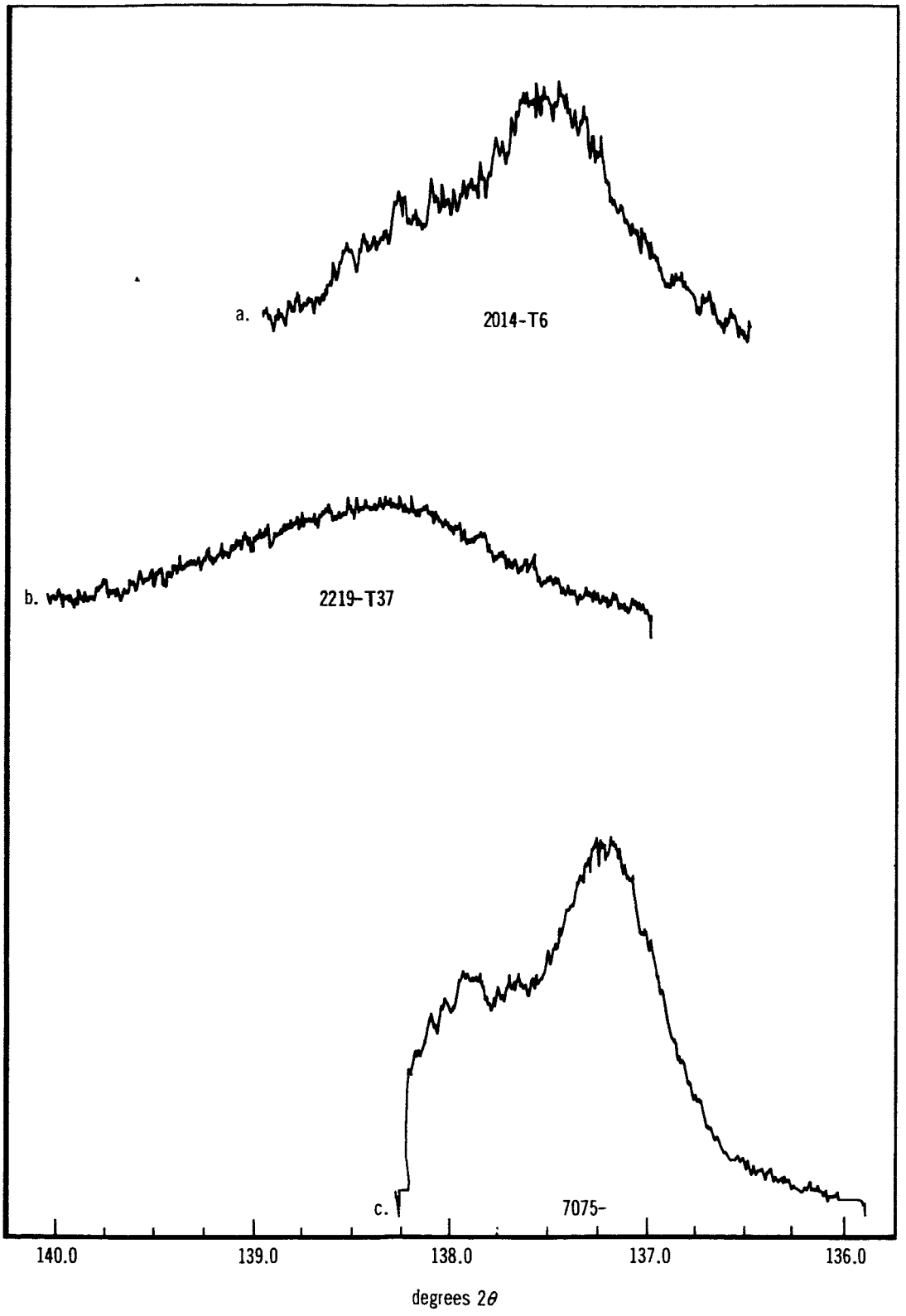

FIGURE 2.–(422) REFLECTION (a) 2014-T6,(b) 2219-T37,(c) 7075-T6

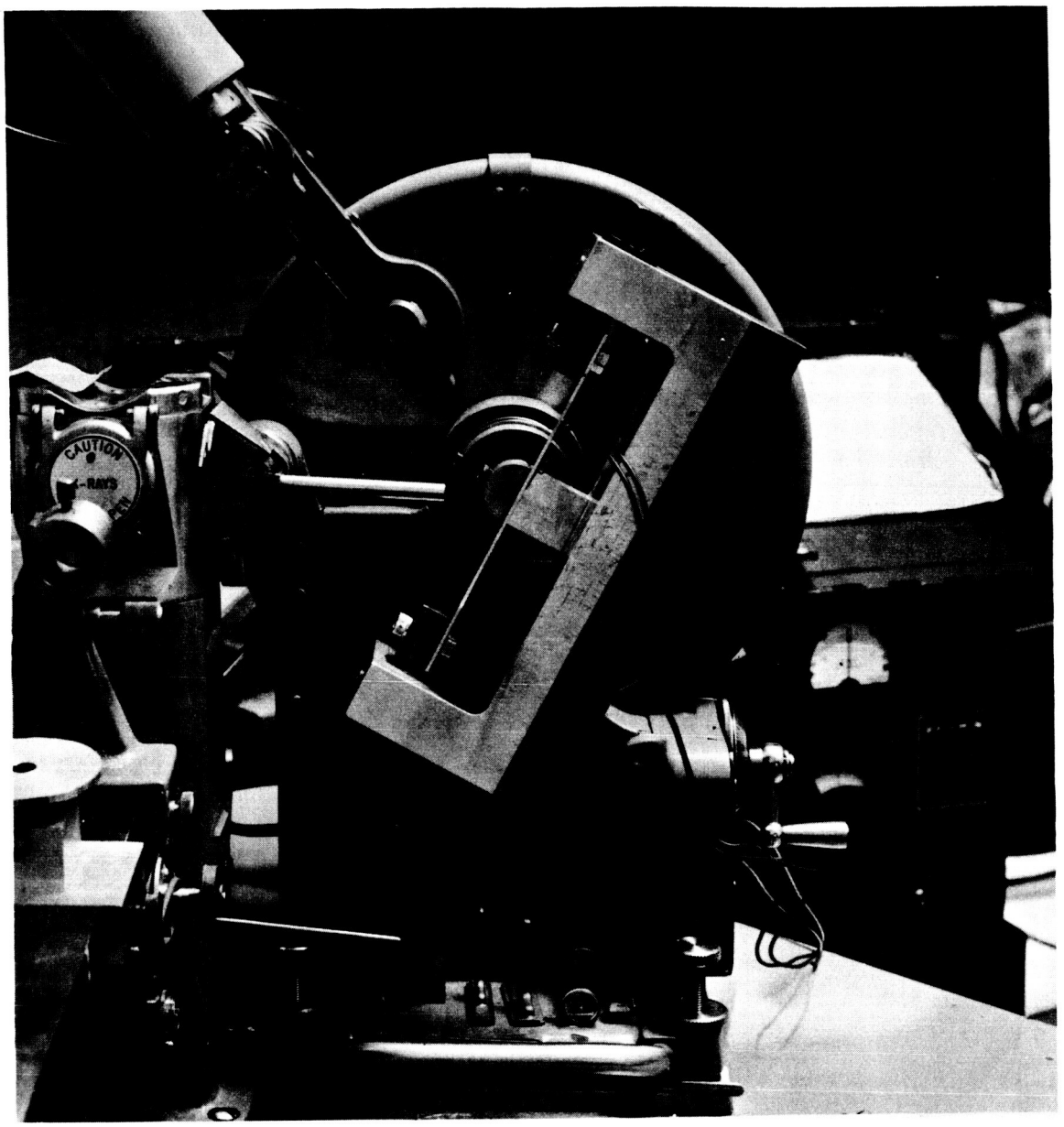

FIGURE 3.- PHOTOGRAPHIC ILLUSTRATION OF THE DIFFRACTOMETER APPARATUS SHOWING UNIAXIAL STRESS FIXTURE

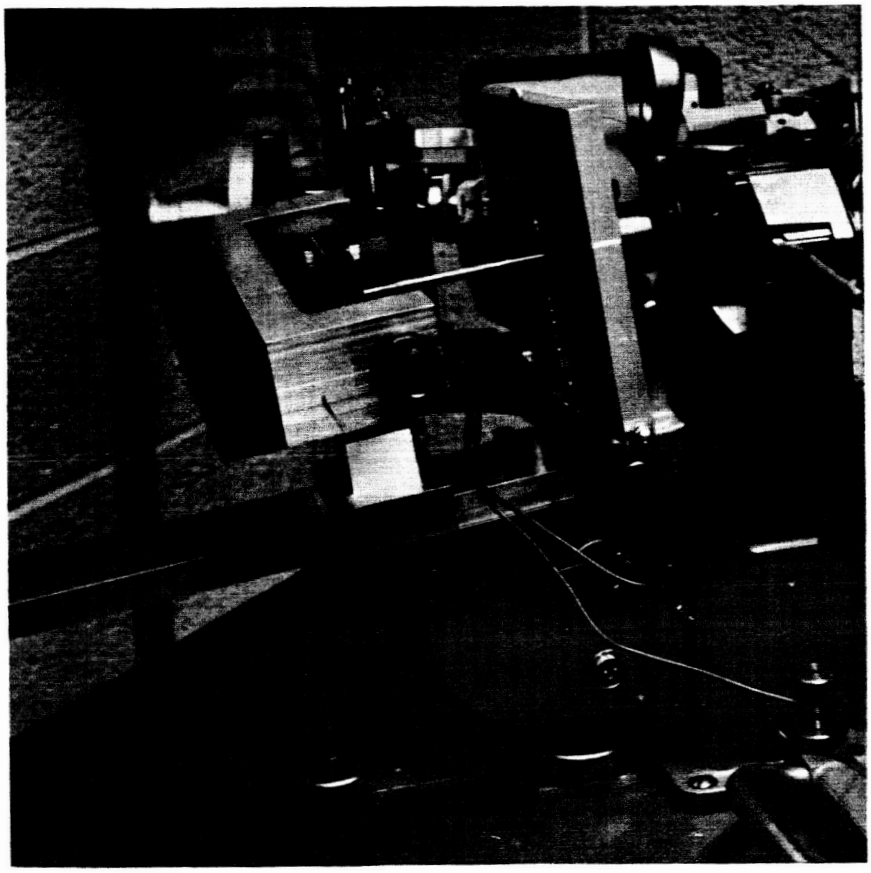

FIGURE 4.-PHOTOGRAPHIC ILLUSTRATION OF THE BACK REFLECTION CAMERA APPARATUS

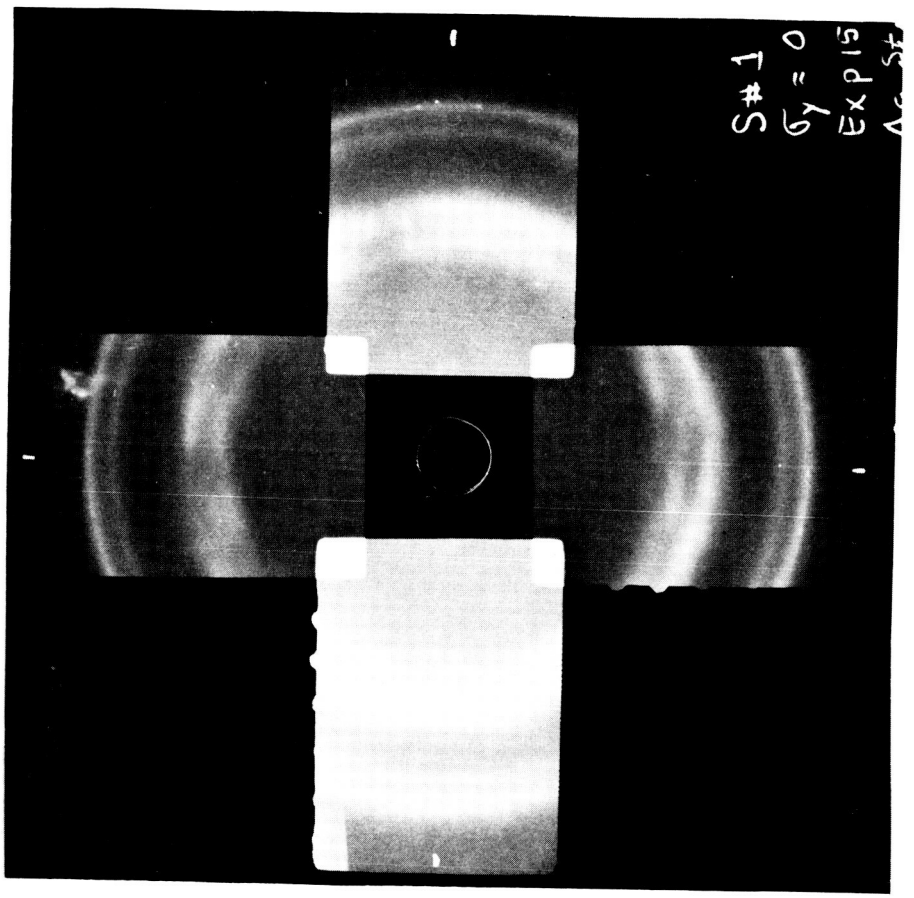

FIGURE 5.- BACK REFLECTION PHOTOGRAPH OF THE (511) (333) ALUMINUM LINE

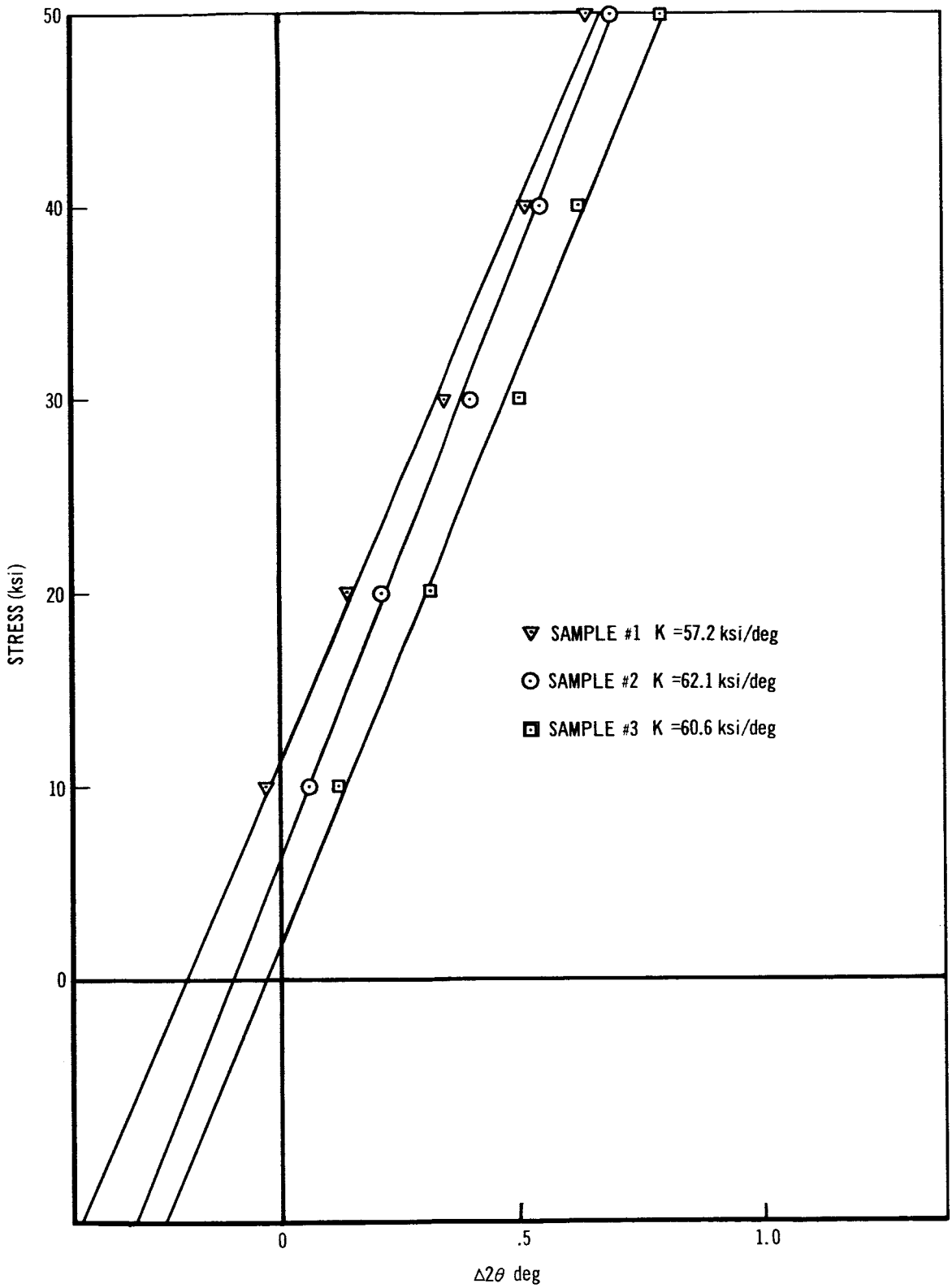

FIGURE 6.- APPLIED STRESS VERSUS $\Delta 2\theta$ FOR 2014-T6 ALLOY SAMPLES

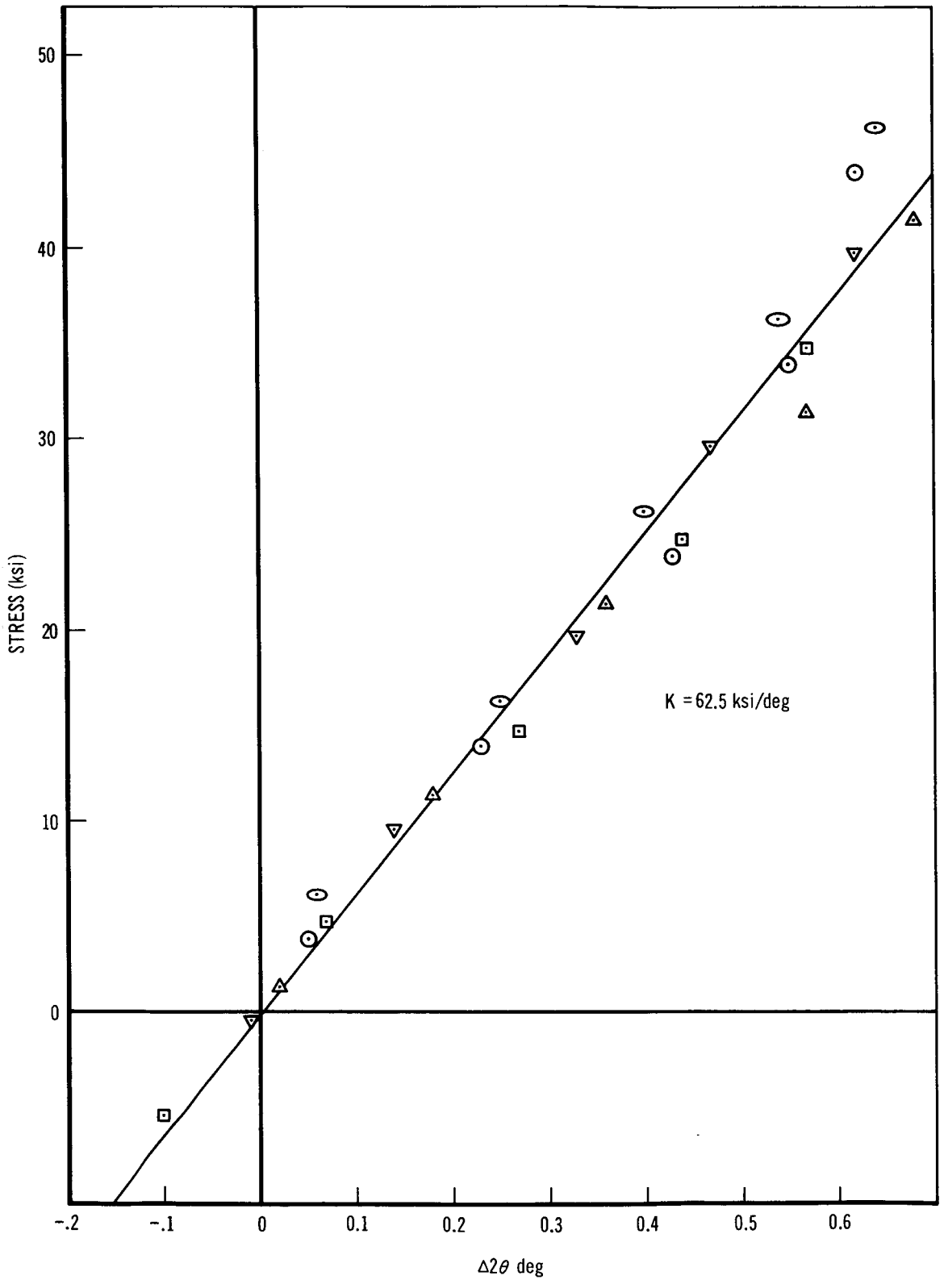

FIGURE 7.–STRESS VERSUS $\Delta 2\theta$ FOR 2014-T6 ALLOY NORMALIZED TO ZERO RESIDUAL STRESS

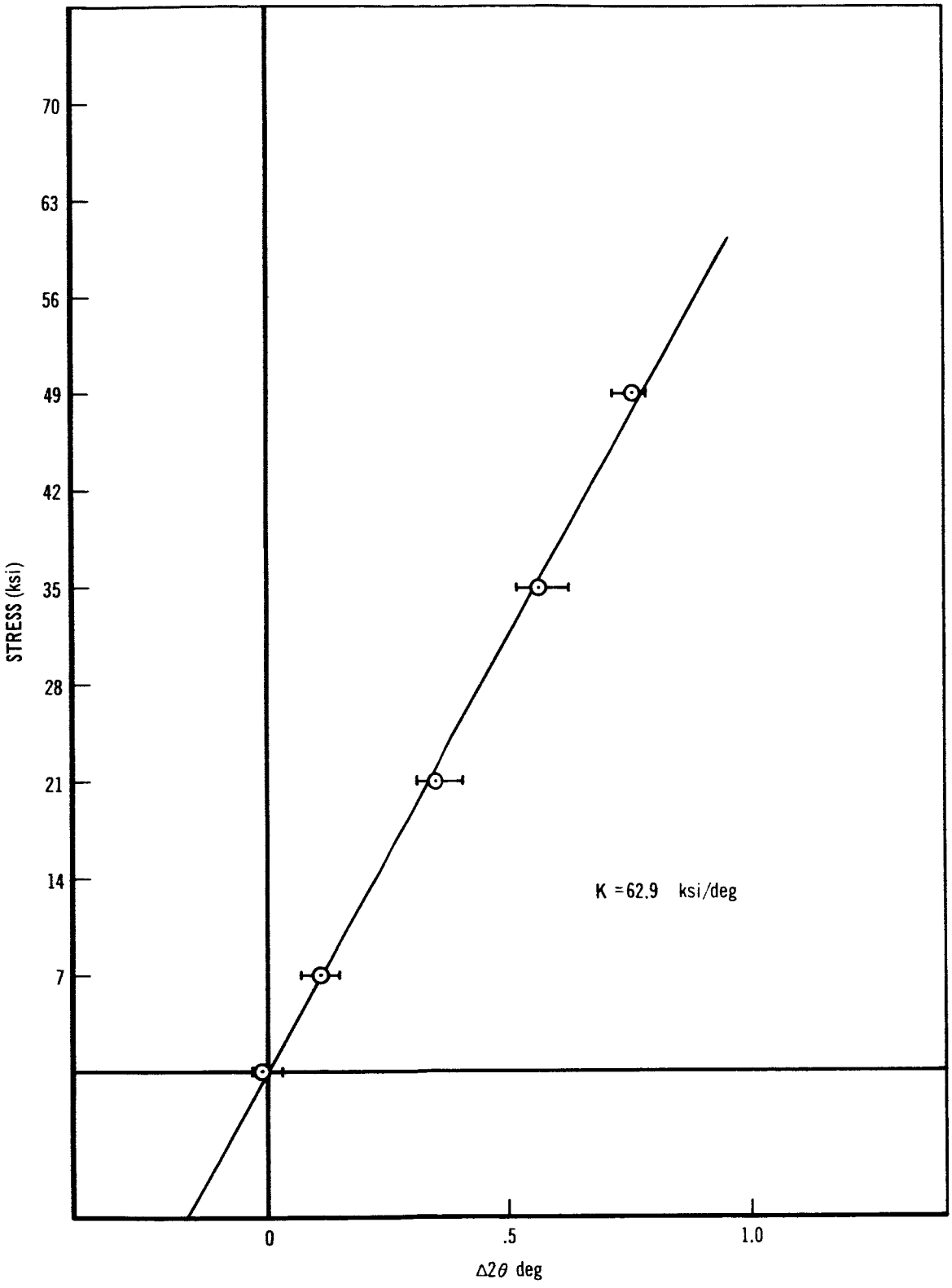

FIGURE 8.–STRESS VERSUS Δ 2 θ FOR 2014-T6 ALLOY SAMPLES WITH ZERO RESIDUAL STRESS

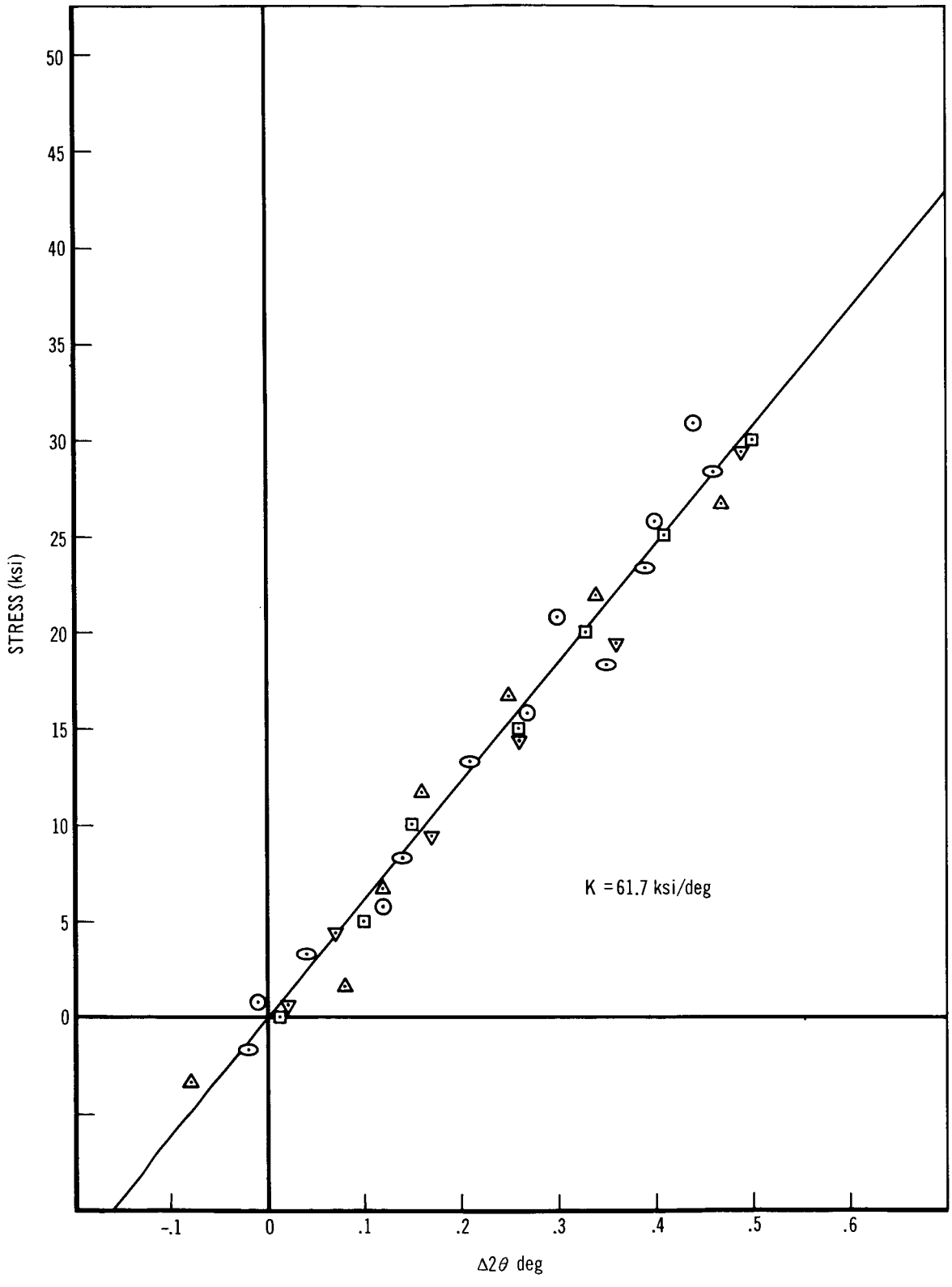

FIGURE 9.- STRESS VERSUS $\Delta 2\theta$ FOR 2219-T37 NORMALIZED TO ZERO RESIDUAL STRESS

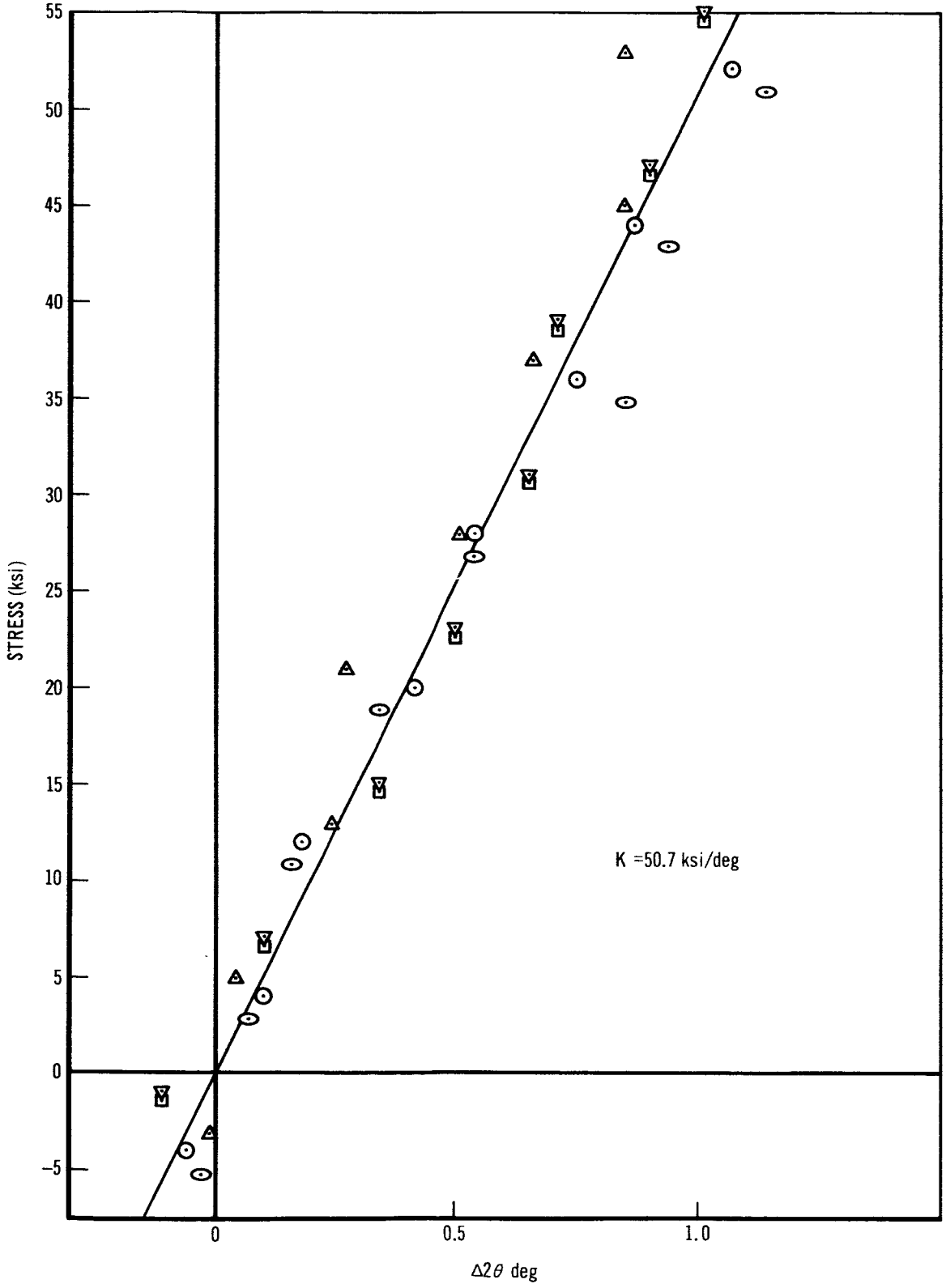

FIGURE 10.-STRESS VERSUS $\Delta 2\theta$ FOR 7075-T6 NORMALIZED TO ZERO RESIDUAL STRESS

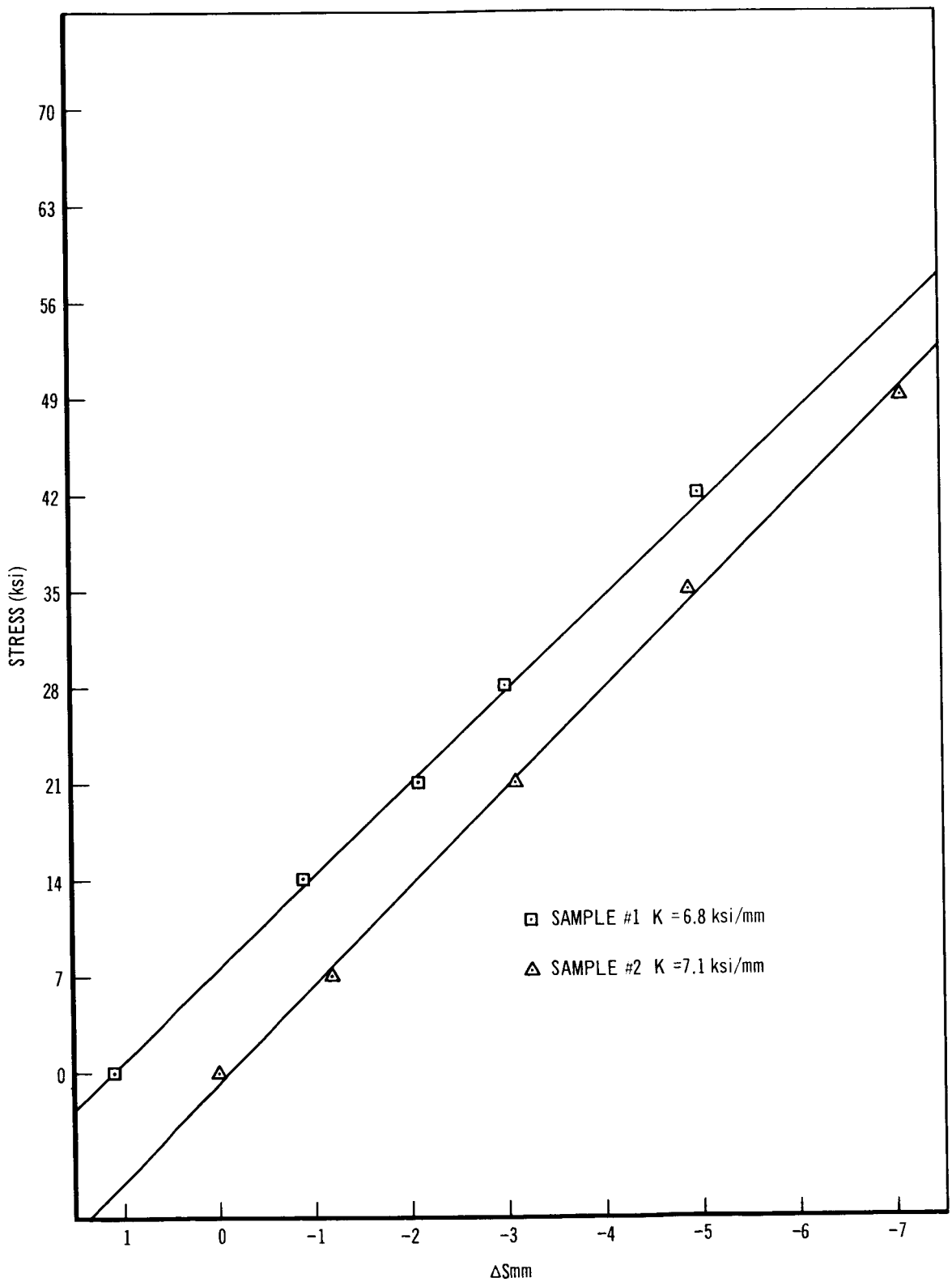

FIGURE 11.- STRESS VERSUS Δ S FOR 2014-T6 SAMPLES INDICATING RESIDUAL STRESS

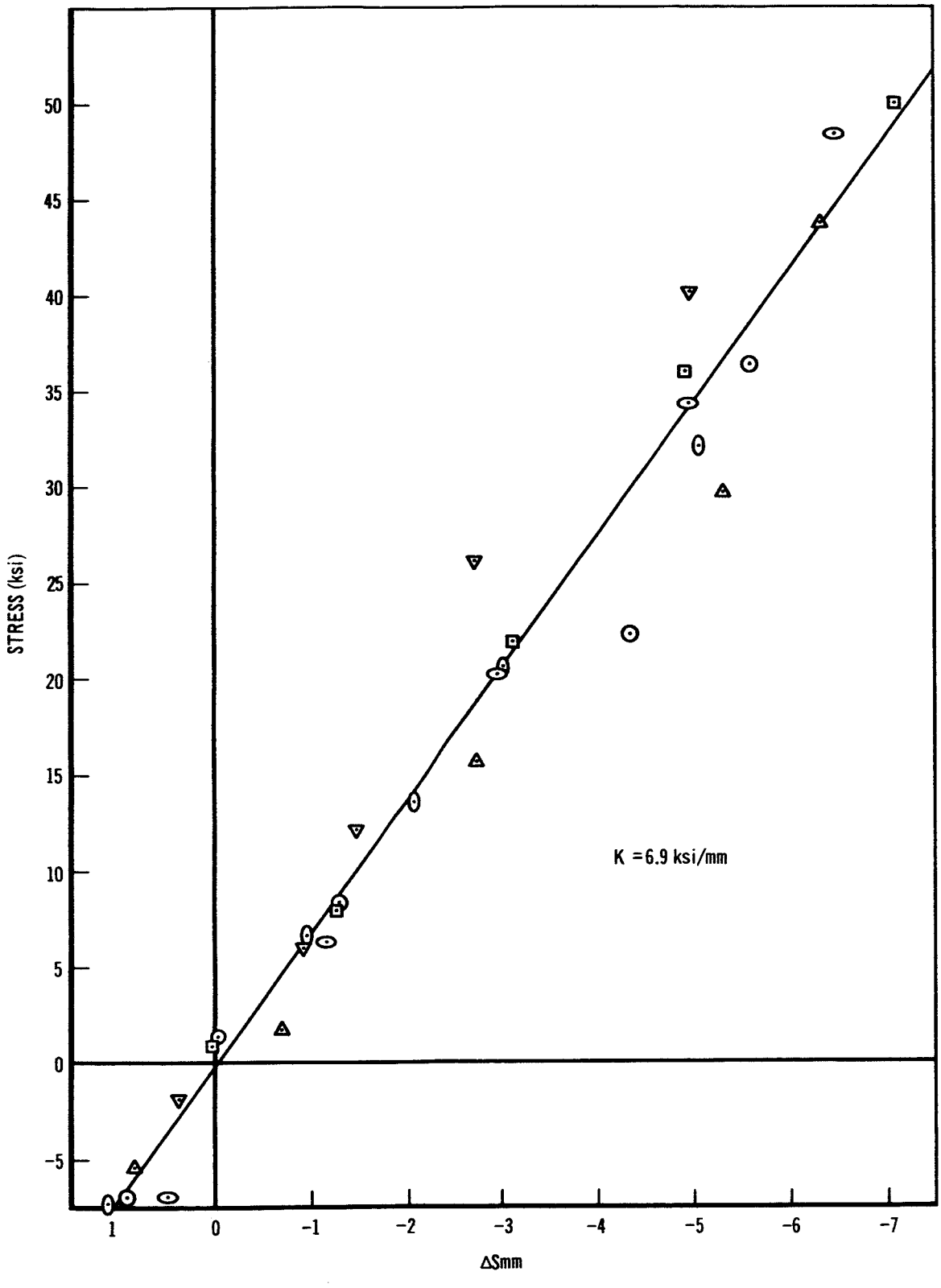

FIGURE 12.–STRESS VERSUS Δ S FOR 2014-T6 ALLOY NORMALIZED TO ZERO RESIDUAL STRESS

APPROVAL

EXPERIMENTAL X-RAY STRESS ANALYSIS FOR PRECIPITATION HARDENED ALUMINUM ALLOYS

By James H. Wharton and William L. Prince
George C. Marshall Space Flight Center

The information in this report has been reviewed for security classification. Review of any information concerning Department of Defense or Atomic Energy Commission programs has been made by the MSFC Security Classification Officer. This report, in its entirety, has been determined to be unclassified.

This document has also been reviewed and approved for technical accuracy.

W. A. RIEHL
Chief, Chemistry Branch

W. R. LUCAS
Chief, Materials Division

for F. B. CLINE
Director, Propulsion and Vehicle Engineering Laboratory

NASA Scientific and Technical Information Facility (25)
P. O. Box 33
College Park, Maryland 20740

R-DIR	Mr. Weidner
R-ASTR-DIR	Dr. Haeussermann
R-ASTR-E	Mr. Fichtner
R-ASTR-N	Mr. Moore
R-ASTR-I	Mr. Hoberg
R-ASTR-R	Mr. Taylor
R-ASTR-M	Mr. Boehm
R-ME-DIR	Mr. Kuers
R-ME-A	Mr. Paetz
R-ME-A	Mr. Nowak
R-ME-D	Mr. Eisenhardt
R-ME-M	Mr. Orr
R-P&VE-DIR	Mr. Cline
R-P&VE-DIR	Mr. Hellebrand
R-P&VE-DIR	Mr. Palaoro
R-P&VE-M	Dr. Lucas (5)
R-P&VE-M	Mr. Holmes
R-P&VE-M	Mr. Zoller
R-P&VE-MC	Mr. Riehl (50)
R-P&VE-ME	Mr. Kingsbury
R-P&VE-MM	Mr. Cataldo
R-P&VE-MMA	Mr. Wagner
R-P&VE-MMC	Mr. Williamson
R-P&VE-MMJ	Mr. Davis
R-P&VE-MMM	Mr. Hess
R-P&VE-MN	Dr. Shannon
R-P&VE-P	Mr. Paul
R-P&VE-S	Mr. Kroll
R-P&VE-V	Mr. Aberg
R-P&VE-VNR	Mr. McDaniel
R-QUAL-DIR	Mr. Grau
R-QUAL-DIR	Mr. Trot
R-QUAL-A	Mr. Henritze
R-QUAL-Q	Mr. Brien
R-QUAL-R	Mr. Chandler
R-QUAL-P	Mr. Brooks
R-TEST-DIR	Mr. Heimburg
LVO-DIR	Dr. Gruene
LVO-M	Mr. Pickett
I-DIR	Dr. Mrazek
I-E-MGR	Mr. Belew
LVO-AD	Mr. Zeiler
R-P&VE-RT	Mr. Hofues
MS-F	Mr. Roberts (3)
MS-H	Mr. Akens
CC-P	Mr. Wofford
MS-T (5)	Mr. Wiggins
MS-IP	Mr. Remer
MS-IPL	Miss Robertson (8)